Journal of Medicinal Chemistry

Article

pubs.acs.org/jmc

Pharmacophoric Modifications Lead to Superpotent αvβ3 Integrin Ligands with Suppressed α5β1 Activity

Stefanie Neubauer,[†,×,#] Florian Rechenmacher,[†,×] Richard Brimioulle,[†] Francesco Saverio Di Leva,[‡,§] Alexander Bochen,[†] Tariq R. Sobahi,[∥] Margret Schottelius,[⊥] Ettore Novellino,[§] Carlos Mas-Moruno,[†,∞] Luciana Marinelli,[§] and Horst Kessler*[,†,∥]

[†]Department Chemie, Institute for Advanced Study (IAS) and Center of Integrated Protein Science (CIPSM), Technische Universität München, Lichtenbergstrasse 4, 85747 Garching, Germany

[‡]Drug Discovery and Development, Istituto Italiano di Tecnologia, Via Morego, 30, 16163 Genova, Italy

[§]Dipartimento di Farmacia, Università di Napoli "Federico II", Via D. Montesano, 49-80131 Napoli, Italy

[∥]Department of Chemistry, Faculty of Science, King Abdulaziz University, P.O. Box 80203, Jeddah 21589, Saudi Arabia

[⊥]Nuklearmedizinische Klinik und Poliklinik, Klinikum Rechts der Isar der Technische Universität München, Ismaninger Strasse 22, 81675 München, Germany

Supporting Information

ABSTRACT: The selective targeting of the αvβ3 integrin subtype without affecting the structurally closely related receptor α5β1 is crucial for understanding the details of their biological and pathological functions and thus of great relevance for diagnostic and therapeutic approaches in cancer treatment. Here, we present the synthesis of highly active RGD peptidomimetics for the αvβ3 integrin with remarkable selectivity against α5β1. Incorporation of a methoxypyridine building block into a ligand scaffold and variation of different functional moieties led to αvβ3-antagonistic activities in the low nanomolar or even subnanomolar range. Furthermore, docking studies were performed to give insights into the binding modes of the novel compounds. The presented library comprises powerful ligands for specific addressing and blocking of the αvβ3 integrin subtype, thereby representing privileged tools for integrin-based personalized medicine.

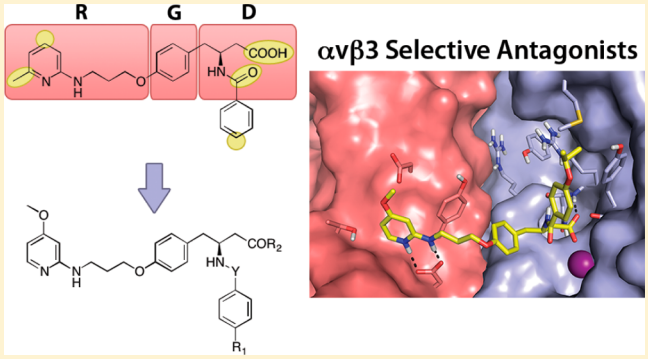

INTRODUCTION

The integrin family, which consists of 24 cell surface receptors, represents a promising target for cancer therapy as well as disease monitoring, since its members enable cell adhesion, proliferation, and survival by interacting with proteins of the extracellular matrix (ECM).[1,2] Integrins are known to be aberrantly up-regulated on various cancer cells and the surrounding tissues compared to normal tissues and thus are key players in tumor progression, pathological angiogenesis, and vascularization.[3] In this way, they are involved in the formation of new blood vessels and guarantee supply of the tumor with oxygen and nutrients. Furthermore, integrins are involved in a plethora of other diseases, such as multiple sclerosis, Crohn's disease, or inflammation.[1−4]

An important subfamily comprises the arginine−glycine−aspartate (RGD)[5] binding integrins, including all αv integrins, the α5β1 subtype, and the blood platelet integrin αIIbβ3.[6] Over the past 2 decades it has been pointed out that αvβ3, αvβ5, and α5β1 are of high relevance in angiogenesis and tumor development, which turned them into attractive targets for medicinal chemistry.[7] We and others have reported the development of linear and cyclic peptides, peptidomimetics, or small molecules with affinity for RGD-based integrins as promising drug candidates to inhibit pathological angiogenesis.[8−17] One of the most prominent integrin targeting drug candidates is cilengitide,[10,18,19] a cyclic pentapeptide with affinity for αvβ3 in the subnanomolar range and for αvβ5 and α5β1 in the low nanomolar range, which is currently undergoing clinical phase II for treatment of several cancer types, such as non-small-cell lung cancer (NSCLC) or prostate cancer, but recently failed in a phase III study to cure glioblastoma.[20] However, the fact that the precise roles of αvβ3 and α5β1 integrins in tumor development are not yet fully understood and that cyclic RGD peptides[21,22] are lacking selectivity to discriminate these two receptors has stimulated extensive research to develop novel integrin subtype specific compounds. Such a differentiation was early achieved to discriminate αv and α5β1 integrins from the platelet integrin αIIbβ3 in head-to-tail cyclic pentapeptides of the general

Received: January 16, 2014
Published: March 23, 2014

   dx.doi.org/10.1021/jm500092w | J. Med. Chem. 2014, 57, 3410−3417

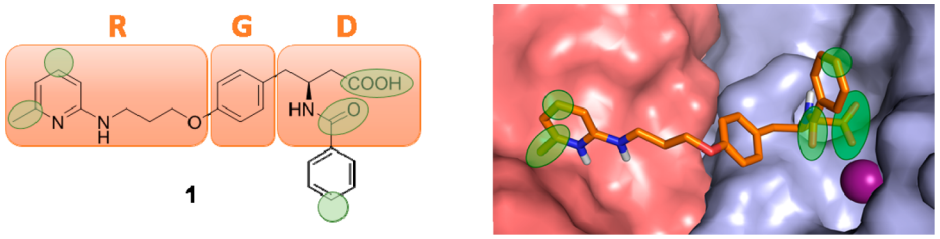

Figure 1. Structure of the $\alpha v\beta 3$-selective compound **1** (left) and its fitting into the binding pocket of $\alpha v\beta 3$ (right). The moieties modified in the molecules of our library are highlighted in green. The metal cation at the MIDAS is represented as a magenta sphere.

Scheme 1. Synthesis Strategy of the $\alpha v\beta 3$-Selective Compounds 2–6[α]

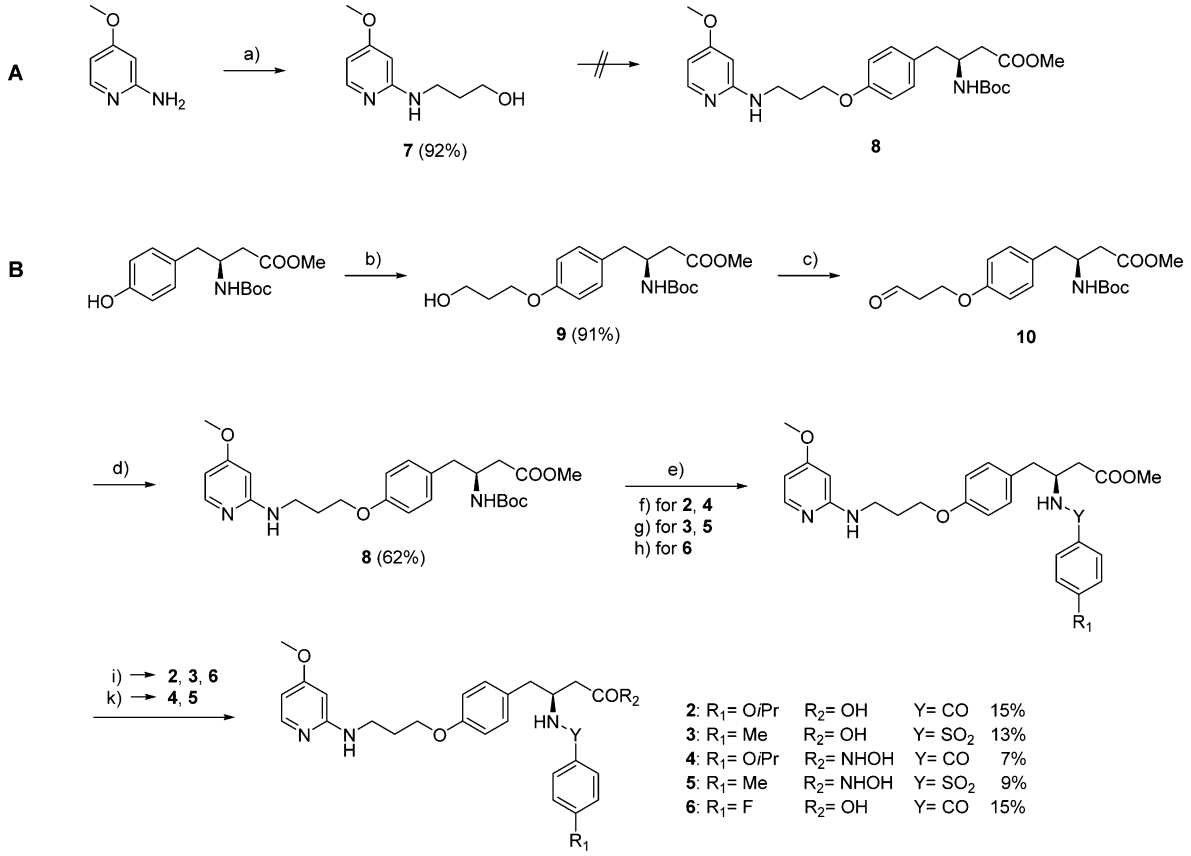

[α]Reagents and conditions: (a) 3-bromopropanol, DMF, 80 °C, 48 h; (b) K_2CO_3, DMF, 0 °C, 30 min, 3-bromopropanol, rt, 16 h; (c) Dess–Martin periodinane, DCM, rt, 3.5 h; (d) 2-amino-4-methoxypyridine, $MgSO_4 \cdot H_2O$, DCM, rt, 1 h, $NaBH(OAc)_3$, overnight; (e) TFA/DCM (1:1, v/v), rt, 1 h; (f) 4-isopropoxybenzoic acid, HATU, DIEA, DMF, rt, overnight; (g) 4-toluenesulfonyl chloride, DIEA, DMF, rt, overnight; (h) 4-fluorobenzoic acid, HATU, DIEA, DMF, rt, overnight; (i) LiOH, $MeOH/H_2O$ (3:1, v/v), rt, overnight; (k) LiOH, NH_2OH_{aq}, THF, rt, overnight.

structure c(RGDfX), containing a D-Phe next to the aspartic acid.[8,23] However, the design of subtype specific molecules for $\alpha v\beta 3$ and $\alpha 5\beta 1$ is of great interest, since it would allow selective targeting and blocking of integrin-mediated signaling cascades under pathological conditions. Furthermore, highly active and selective integrin ligands would pave the way for developing novel tools to investigate their biological roles in vitro as well as in vivo. Nonetheless, the design of these antagonists is challenging because of the similarity in the RGD binding pockets of $\alpha v\beta 3$ and $\alpha 5\beta 1$ (>50%), respectively.[24,25] In this context, peptidomimetics offer certain advantages in comparison to peptides because they enable incorporation of unnatural amino acids and other building blocks to achieve a proper fitting of the molecule into the desired RGD binding pocket.

In the past, we have reported several $\alpha v\beta 3$-active compounds endowed with a satisfactory selectivity profile against the $\alpha 5\beta 1$ integrin subtype.[12] Out of these molecules, one of the most active and selective ligands (compound **1**, Figure 1) was selected and functionalized for surface coating experiments as well as for tumor imaging. However, the results of these studies showed that the compounds were not potent enough to be used for in vivo applications (data not shown).

Herein we report on a library of $\alpha v\beta 3$ integrin antagonists showing activities in the low nanomolar or even subnanomolar range with remarkable selectivity against $\alpha 5\beta 1$. These compounds were designed based on pharmacophoric requirements obtained from previously described $\alpha v\beta 3$-selective or $\alpha v\beta 3/\alpha 5\beta 1$-biselective ligands (Figure 1).[12,26,27] We incorporated a methoxypyridine residue and additionally modified

dx.doi.org/10.1021/jm500092w | J. Med. Chem. 2014, 57, 3410–3417

distinct moieties to optimize the fitting of the ligands into the $\alpha v\beta 3$ integrin binding pocket. Because of the improved activity profile and the possibility of functionalization without losing affinity, we obtained powerful antagonists for coating of surfaces[28,29] or for positron emission tomography (PET) imaging.[30] Moreover, the binding modes of these compounds at the $\alpha v\beta 3$ and $\alpha 5\beta 1$ receptors were carefully investigated through molecular docking studies.

RESULTS AND DISCUSSION

In our previous studies we demonstrated that a β-homotyrosine backbone in RGD peptidomimetics is essential to gain activity toward the $\alpha v\beta 3$ integrin and selectivity against $\alpha 5\beta 1$ and $\alpha IIb\beta 3$.[12] Besides the carboxylate group of tyrosine, which acts as a mimic of the aspartate and coordinates a divalent metallic cation at the metal-ion-dependent adhesion site (MIDAS) in the RGD binding site, the basic moiety, the pyridine residue of **1**, is also essential as an arginine surrogate (Figure 1). The modification of this basic moiety is particularly important to improve the affinity toward $\alpha v\beta 3$ because of peculiar steric and electrostatic demands imposed by the amino acid residues present in the RGD binding region of the α-subunits. In this regard, it has been already demonstrated that the substitution in the para-position of the pyridine ring shows a greater influence on the activity than in any other positions of the aromatic system.[12] In our design strategy, we aimed at introducing a methoxy group in the para-position to enhance the pyridine basicity, thus favoring the recognition by the RGD binding region of the αv-subunits, which is more "acidic" than that of $\alpha 5\beta 1$.[24] Thus, our first approach comprised the incorporation of a *p*-methoxy group[31,32] into the basic pyridine ring of **1**.

Starting from the commercially available 2-amino-4-methoxypyridine, we first performed a nucleophilic substitution with 3-bromo-1-propanol to build up the new ligands according to a reported strategy (Scheme 1A).[12] However, the well-established Mitsunobu reaction[26] of the resulting alcohol **7** and the protected β-homotyrosine ester[26] failed to yield the scaffold **8**. Extensive studies concerning the synthetic strategy and reaction conditions (e.g., various nucleophilic substitutions with improved leaving groups) finally led to a reverse synthetic route starting with β-homotyrosine instead of the pyridine derivative (Scheme 1B). First, a nucleophilic substitution was performed with the protected β-homotyrosine ester and 3-amino-1-propanol following a standard procedure with K_2CO_3 in DMF to obtain the alcohol **9** in excellent yields (Scheme 1B). Afterward, **9** was oxidized with Dess–Martin periodinane in DCM[33] to obtain the aldehyde **10**, which was directly used in the next step without further purification. To introduce the 2-amino-4-methoxypyridine building block, we performed a reductive amination of **10** in the presence of magnesium sulfate and sodium triacetoxyborohydride in DCM[33] in order to yield **8** as backbone and lead structure for the development of the new peptidomimetics **2**–**6**.

Previous studies on $\alpha 5\beta 1$-selective compounds revealed that introduction of a sulfonamide bond (Y = SO_2, Scheme 1) instead of a carboxamide (Y = CO, Scheme 1) at the amino group of β-tyrosine-based peptidomimetics can enhance their affinity because of different structural orientations of the aromatic residue.[12,26] On the basis of this observation, we investigated this effect on $\alpha v\beta 3$ antagonists. Hence, after Boc-deprotection of **8** under acidic conditions, the free amine was acylated with either 4-isopropoxybenzoic acid or 4-toluenesulfonyl chloride, followed by saponification of the methyl ester to obtain the deprotected carboxylic acids **2** and **3**, respectively. In a competitive integrin binding ELISA[34] (see Supporting Information) both compounds displayed outstanding subnanomolar activities for $\alpha v\beta 3$, improved by more than 1 order of magnitude in comparison to the reference compound **1** (Table 1). Besides their potent antagonistic activities, these compounds also showed good selectivities against $\alpha 5\beta 1$ and the platelet integrin $\alpha IIb\beta 3$ (>10000 nM).

Table 1. Activity Profiles of the Synthesized $\alpha v\beta 3$-Selective Antagonists 1–6[a]

	IC_{50} (nM)		
compd	$\alpha v\beta 3$	$\alpha 5\beta 1$	$\alpha IIb\beta 3$
1[b]	110 ± 64	>10000	nd
2	0.86 ± 0.06	126.5 ± 25.6	>10000
3	0.65 ± 0.05	108.0 ± 27.5	>10000
4	638 ± 124	>10000	nd
5	75.1 ± 8.6	>10000	nd
6	1.6 ± 0.17	64.2 ± 13.1	nd
cilengitide	0.54 ± 0.02	15.4 ± 3	>1000

[a]All IC_{50} values were determined in a solid phase integrin binding ELISA[34] and referenced to cilengitide.[10,18] nd: not determined. [b]Compound **1** was synthesized according to the literature and originally tested by the Jerini AG, Berlin, Germany, with a slightly different method (13 nM for $\alpha v\beta 3$ and 3946 nM for $\alpha 5\beta 1$).[12]

Comparing compounds **2** and **3**, the first one turned out to be the most promising compound for further functionalization, as it can be modified in a very straightforward manner through the introduction of different functional moieties at the para-position of the aromatic carboxylic acid building block. In order to explore the affinity profile toward other RGD-binding integrins, we determined the IC_{50} values of **2** toward the $\alpha v\beta 5$ and $\alpha v\beta 6$ subtypes. In comparison to the subnanomolar antagonistic activity observed for $\alpha v\beta 3$, compound **2** showed a lower affinity for $\alpha v\beta 6$ (IC_{50} of 20 nM) and a good selectivity against $\alpha v\beta 5$ (IC_{50} of 227 nM) (see Supporting Information, Table S1). Moreover, we have already shown that this ligand can be functionalized and used for coating gold and titanium-based biomaterials in vitro and for selective tumor imaging in vivo with outstanding results.[28−30,35]

After the incorporation of the methoxypyridine moiety, we investigated the effects of changing the ligand scaffold length by replacing the carboxylic acid moiety, responsible for the crucial interaction with the metal cation at the MIDAS,[36] with a larger functional group. For this reason, we synthesized ligands with a hydroxamic acid. This functionality, in contrast to carboxylic acids, is not charged under neutral pH conditions and often has shown better pharmacodynamic behaviors.[37] Thus, the methyl ester of the β-tyrosine scaffold was converted into the hydroxamic acid following a modified procedure[37,38] with hydroxylamine to render compounds **4** and **5**. This protocol simultaneously favors both the saponification of the methyl ester and the final conversion of the carboxylate to the corresponding hydroxamic acid. To minimize saponification, the addition of LiOH to the reaction mixture of THF/water and hydroxylamine was reduced to less than 1 equiv of LiOH. Although these compounds (**4** and **5**) display excellent selectivities against $\alpha 5\beta 1$, their activities toward $\alpha v\beta 3$ were significantly reduced compared to the analogues **2** and **3**.

In a final approach, the scaffold **8** was modified with a fluorine atom through coupling with *p*-fluorobenzoic acid

dx.doi.org/10.1021/jm500092w | J. Med. Chem. 2014, 57, 3410−3417

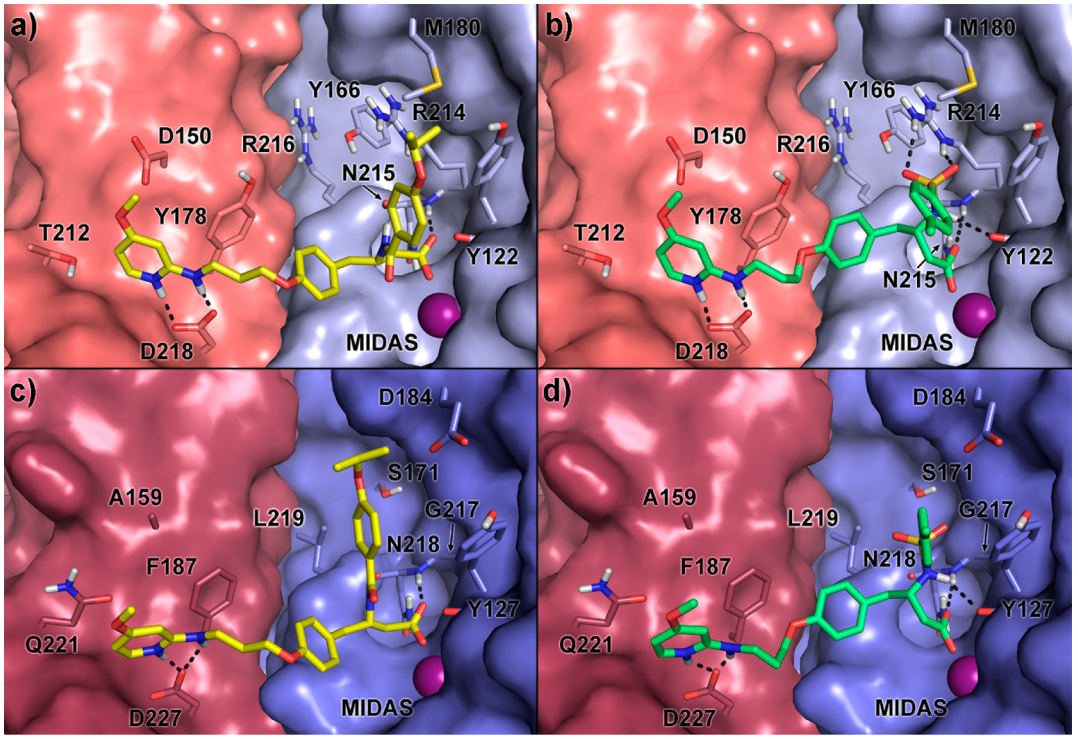

Figure 2. Binding modes of **2** (a, c) and **3** (b, d) at the $\alpha v\beta 3$ and $\alpha 5\beta 1$ integrins. **2** and **3** are shown as yellow and green sticks, respectively. The αv and $\beta 3$ subunits are depicted as pink and light blue surfaces (upper panels a and b), while the $\alpha 5$ and $\beta 1$ subunits are depicted as red and blue surfaces (lower panels c and d). Receptor amino acid side chains important for the ligand binding are represented as sticks. The metal cation at the MIDAS is represented as a magenta sphere.

according to a standard procedure.[39] Compound **6** showed excellent activity for $\alpha v\beta 3$ (1.6 nM) and good selectivity against $\alpha 5\beta 1$. Thus, labeling with ^{18}F would be a feasible strategy to selectively target and image $\alpha v\beta 3$ integrins via PET.[40]

To rationalize the structure−activity relationships as well as the selectivity profiles of the new $\alpha v\beta 3$-binding peptidomimetics, molecular modeling studies were performed by docking the most active compounds **2** and **3** into the binding site of $\alpha v\beta 3$[41] and $\alpha 5\beta 1$[24] integrins (for docking methods, see the Supporting Information). According to docking results, compounds **2** and **3** bind to the $\alpha v\beta 3$ RGD binding site in a similar fashion (Figure 2). For both ligands, the carboxylate group coordinates the metal ion at the MIDAS and also forms a hydrogen bond with the backbone NH group of ($\beta 3$)-Asn215. On the opposite side, the positively charged 2-amino-4-methoxypyridine moiety salt-bridges with (αv)-Asp218 and establishes a $\pi-\pi$ interaction with the (αv)-Tyr178 side chain. Moreover, the β-homotyrosine scaffold is found in the proximity of (αv)-Tyr178, thus establishing parallel-displaced $\pi-\pi$ interactions with the aromatic side chain of this residue. The only difference observed in the binding modes of **2** and **3** resides in the interaction patterns between the *p*-isopropyloxyphenyl moiety of **2** and the *p*-methylbenzenesulfonamide group of **3**, respectively, owing to the distinctive structural features of these substituents. The *p*-isopropyloxyphenyl moiety extends toward the specificity determining loop (SDL) of the integrin binding pocket, leading to a T-shape interaction with ($\beta 3$)-Tyr122, a cation$-\pi$ interaction with ($\beta 3$)-Arg214, and lipophilic contacts with the ($\beta 3$)-Met180 side chain. Alternatively, the *p*-methylbenzenesulfonamide group of **3** is predicted to additionally establish a T-shape interaction with the ($\beta 3$)-Tyr122 side chain and to form a hydrogen bond with the ($\beta 3$)-Arg214 side chain through its oxygen atoms and with the backbone CO group of ($\beta 3$)-Tyr122 through its NH group. Overall, the docking poses predicted for **2** and **3** at the $\alpha v\beta 3$ RGD binding site are useful to explain the subnanomolar activities displayed by these ligands toward this integrin subtype. Furthermore, it is worth noting that the substitution of the 6-methyl group in our reference compound **1** with the electron-donating 4-methoxy group enhances the basicity of the pyridine ring and also reduces at minimum its steric clash with (αv)-Thr212. These effects allow the basic moiety to properly interact with (αv)-Asp218, increasing the affinity of the new analogues for the $\alpha v\beta 3$ receptor. For opposite reasons (i.e., enhanced steric clash with (αv)-Thr212), the elongation of the ligand main chain through the replacement of the carboxylic moiety with a hydroxamate group turned out to be detrimental for the $\alpha v\beta 3$ antagonism, as observed for compounds **4** and **5**. Indeed, the optimal distance between the acidic and the basic moieties in $\alpha v\beta 3$ integrin ligands is ~13 Å,[27] as in the case of our carboxylic compounds, while this distance is higher in hydroxamic derivatives which are too long for properly fitting in the RGD binding cavity.[12]

Finally, the slightly lower affinity of the carboxylic derivative **6** toward $\alpha v\beta 3$, if compared to **2**, is mainly ascribable to the loss of favorable lipophilic contacts with the ($\beta 3$)-Met180 side chain due to the replacement of the *p*-isopropoxy group at the phenyl ring with a tiny and more polar fluorine atom.

The lower potencies of the newly synthesized peptidomimetics toward the $\alpha 5\beta 1$ receptor with respect to $\alpha v\beta 3$ are due to single point mutations that differentiate the binding cavities of these two integrin subtypes (Figure 2).[12,24,27,37] In the α subunit, the acidic (αv)-Asp150 is mutated to the nonpolar ($\alpha 5$)-Ala159, and (αv)-Thr212 is replaced by the bulkier ($\alpha 5$)-

dx.doi.org/10.1021/jm500092w | J. Med. Chem. 2014, 57, 3410−3417

Gln221. Interestingly, the presence of the Gln residue reduces the space available for the binding of the basic moiety, as clearly shown by docking of **2** and **3** into the $\alpha5\beta1$ RGD binding site, thus leading to a decrease in affinity of these two ligands toward this integrin subtype. This tendency is even more evident for the hydroxamic derivatives **4** and **5**, in which, as previously reported, the distance between the metal-coordinating acidic group and the basic moiety is increased. In addition, the binding region on the $\alpha5$ subunit is less acidic than that found at the αv subunit due to the mutation of (αv)-Asp150 to ($\alpha5$)-Ala159. In this regard, the insertion of more basic groups generally results in less potent $\alpha5\beta1$ antagonists.[12,24,25,27,37] Thus, the introduction of the electron-donating 4-methoxy group, which increases the basicity of the pyridine ring, lowers the affinity of the ligands toward the $\alpha5\beta1$ integrin. In the β subunit, the substitution of the ($\beta3$)-Arg214 residue with ($\beta1$)-Gly217 is predicted to affect the binding affinity of both **2** and **3**. In particular, in the $\alpha5\beta1$ receptor the oxygen atoms of the sulfonamide moiety of **3** cannot establish the same H-bonds as observed in $\alpha v\beta3$, while the *p*-isopropyloxyphenyl ring of **2** misses an important cation$-\pi$ interaction. In the case of **2**, the substitution of the lipophilic ($\beta3$)-Met180 with the acidic ($\beta1$)-Asp184 might also contribute to reduce the ligand affinity toward $\alpha5\beta1$, since the *p*-isopropyloxyl substituent of the phenyl ring cannot form any favorable hydrophobic contacts with Asp, contrary to what is observed in $\alpha v\beta3$. Conversely, the presence of the more polar fluorine atom on **6** allows this ligand to retain satisfactory selectivity against $\alpha5\beta1$.

CONCLUSION

We have developed a small library of RGD peptidomimetics based on a β-homotyrosine scaffold as new $\alpha v\beta3$ integrin antagonists. These compounds incorporate a basic methoxypyridine moiety and present different metal-coordinating acidic groups and aromatic building blocks. Competitive in vitro assays have demonstrated that two of these ligands, namely, **2** and **3**, are highly potent binders of the $\alpha v\beta3$ integrin, displaying IC_{50} values in the subnanomolar range. Furthermore, they show a high selectivity against the $\alpha5\beta1$ receptor. Molecular docking studies have identified the binding modes of **2** and **3** at both the $\alpha v\beta3$ and $\alpha5\beta1$ receptors, disclosing the molecular requisites for achieving optimal activity and selectivity toward these integrin subtypes. These studies therefore provide useful insights to improve the design of new integrin-selective peptidomimetics ligands, which are excellent candidates for medical and biophysical applications.

EXPERIMENTAL SECTION

Chemistry. Solvents were purchased from Aldrich, Fluka, Merck, and Prolabo. Reactions sensible to oxygen or water were performed in flame-dried reaction vessels under an argon atmosphere (99.996%). Coupling reagents were purchased from Iris Biotech GmbH and Medalchemy. All other chemicals and organic solvents were purchased from commercial suppliers at the highest purity available and used without further purification. Flash chromatographic purification was performed using silica gel 60 (40−63 μm) from Merck at 1−1.5 atm pressure.

Analytical high-performance liquid chromatography (HPLC) was performed using an Amersham Pharmacia Biotech Äkta Basic 10F equipment with a P-900 pump system, a reversed-phase YMC-ODS-A C18 column (4.6 mm × 250 mm, 5 μm), and UV detection (UV-900, 220 and 254 nm). The system was run at a flow rate of 1 mL/min over 30 min using H_2O (0.1% (v/v) TFA) and MeCN (0.1% (v/v) TFA) as solvents. Semipreparative HPLC was carried out on a Beckmann instrument (system gold, solvent delivery module 126, UV detector 166) using an YMC ODS-A column (20 mm × 250 mm, 5 μm), with a flow rate of 8 mL/min. Linear gradients using H_2O (0.1% (v/v) TFA) and MeCN (0.1% (v/v) TFA) were run over varying periods of time. HPLC−mass spectrometry (MS) analyses were performed on a Hewlett-Packard series HP 1100 with a Finnigan LCQ mass spectrometer using a YMC Hydrosphere C18 column (2.1 mm × 125 mm, 3 μm). The system uses H_2O (0.1% (v/v) formic acid) and MeCN (0.1% (v/v) formic acid) as eluents. High resolution mass spectrometry (HR-MS) was recorded on a Thermo Finnigan LTQ-FT (ESI-ICR) spectrometer. ^{1}H NMR and ^{13}C NMR spectra were recorded at 295 K on a 500 MHz Bruker DMX, 360 MHz Bruker AV, or a 250 MHz Bruker AV spectrometer (Bruker, Karlsruhe, Germany). Chemical shifts (δ) are given in parts per million (ppm). The following solvent peaks were used as internal standards: DMSO-d_6, 2.50 ppm (^{1}H NMR) and 39.52 ppm (^{13}C NMR); $CHCl_3$, 7.26 ppm (^{1}H NMR) and 77.16 ppm (^{13}C NMR).[42] The yields of the syntheses are not optimized. All synthesized compounds exhibit ≥95% purity determined with HPLC−MS.

Boc-Deprotection and Acylation by Aromatic Benzylic Acids (GP1a). The Boc-protected starting material was dissolved in a mixture of TFA and DCM (1:1 (v/v), ∼0.1 M). After stirring for 1 h at room temperature, the solvent was removed under reduced pressure. The resulting deprotected amine was redissolved in DMF (∼0.1 M) followed by addition of the corresponding aromatic acid (1.3 equiv), HATU (1.3 equiv), and DIEA (5 equiv). The resulting yellow solution was stirred overnight at room temperature and the solvent was evaporated.

Boc-Deprotection and Acylation by Aromatic Sulfonyl Chlorides (GP1b). The Boc-protected starting material was dissolved in a mixture of TFA and DCM (1:1; (v/v) ∼0.1 M). After the mixture was stirred for 1 h at room temperature, the solvent was removed under reduced pressure. The resulting deprotected amine was redissolved in DMF (∼0.1 M) followed by addition of the 4-toluenesulfonyl chloride (1.3 equiv) and DIEA (5 equiv). The resulting yellow solution was stirred overnight at room temperature, and the solvent was evaporated.

Saponification of Methyl Ester (GP2a). The residue was dissolved in methanol/water (3:1, v/v), and LiOH (5 equiv) was added to this solution, which was left under stirring at room temperature overnight. The resulting deprotected compound was purified using (semi)preparative reversed phase HPLC and lyophilized to yield a colorless solid.

Formation of Hydroxamic Acid (GP2b). The residue was dissolved in THF, and then LiOH (<1 equiv) and hydroxylamine (50 wt % solution in water) were added to the mixture, which was left under stirring at room temperature overnight. The resulting deprotected compound was purified using (semi)preparative reversed phase HPLC and lyophilized to yield a colorless solid.

(*S*)-3-Benzamido-4-(4-(3-((6-methylpyridin-2-yl)amino)-propoxy)phenyl)butanoic Acid (1). Compound **1** was synthesized according to the literature.[12] ^{1}H NMR and ^{13}C NMR spectra were identical to those previously reported.[12] HPLC (10−90%): t_R = 14.95 min. MS (ESI): m/z (%) = 448.4 $[M + H]^+$.

(*S*)-3-(4-Isopropoxybenzamido)-4-(4-(3-((4-methoxypyridin-2-yl)amino)propoxy)phenyl)butanoic Acid (2). The Boc-deprotection and acylation of the ligand precursor **8** (0.34 g, 0.71 mmol) with 4-isopropoxybenzoic acid (0.17 g, 0.92 mmol) were done according to GP1a. The crude product was saponified according to GP2a. Purification yielded compound **2** (55.6 mg, 0.11 mmol, 15%) as TFA salt. ^{1}H NMR (500 MHz, DMSO): δ [ppm] = 12.87 (bs, 1H), 12.17 (bs, 1H), 8.28 (bs, 1H), 8.13 (d, ^3J = 8.3 Hz, 1H), 7.80 (d, ^3J = 7.1 Hz, 1H), 7.72 (d, ^3J = 8.8 Hz, 2H), 7.13 (d, ^3J = 8.5 Hz, 2H), 6.94 (d, ^3J = 8.8 Hz, 2H), 6.83 (d, ^3J = 8.6 Hz, 2H), 6.46 (dd, ^3J = 7.0 Hz, ^4J = 2.1 Hz, 1H), 6.33 (d, ^4J = 1.9 Hz, 1H), 4.72−4.65 (m, 1H), 4.44−4.37 (m, 1H), 4.01 (t, ^3J = 6.0 Hz, 2H), 3.86 (s, 3H), 3.46−3.42 (m, 2H), 2.80 (dd, ^2J = 13.6 Hz, ^3J = 8.0 Hz, 1H), 2.73 (dd, ^2J = 13.6 Hz, ^3J = 5.8 Hz, 1H), 2.52−2.48 (m, 1H), 2.41 (dd, ^2J = 15.4 Hz, ^3J = 6.2 Hz, 1H), 2.02−1.97 (m, 2H), 1.27 (d, ^3J = 6.0 Hz, 6H). ^{13}C NMR (125 MHz, DMSO): δ [ppm] = 172.5, 165.1, 159.7, 156.8, 130.9,

dx.doi.org/10.1021/jm500092w | J. Med. Chem. 2014, 57, 3410−3417

130.1, 129.0, 126.5, 114.7, 114.1, 103.9, 99.4, 69.3, 64.6, 56.4, 48.3, 40.1, 39.8, 38.7, 27.9, 21.7. HPLC (10−90%): t_R = 17.63 min. MS (ESI): m/z (%) = 522.4 $[M + H]^+$. HR-MS (ESI) ($C_{29}H_{36}N_3O_6^+$) calcd, 522.259 86; found, 522.257 95.

(*S*)-4-(4-(3-((4-Methoxypyridin-2-yl)amino)propoxy)phenyl)-3-(4-methylphenylsulfonamido)butanoic Acid (3). The Boc-deprotection and acylation of the ligand precursor **8** (0.34 g, 0.71 mmol) with 4-toluenesulfonyl chloride (0.16 g, 0.92 mmol) followed GP1b. The crude product was deprotected according to GP2a. Purification yielded compound **3** (47.4 mg, 92.2 μmol, 13%) as TFA salt. ^{1}H NMR (500 MHz, $CDCl_3$): δ [ppm] = 9.42 (bs, 1H), 7.64 (d, ^3J = 8.2 Hz, 2H), 7.59 (d, ^3J = 7.1 Hz, 1H), 7.22 (d, ^3J = 8.0 Hz, 2H), 6.92 (d, ^3J = 8.5 Hz, 2H), 6.71 (d, ^3J = 8.5 Hz, 2H), 6.28 (dd, ^3J = 7.1 Hz, ^4J = 2.3 Hz, 1H), 6.01 (d, ^4J = 2.1 Hz, 1H), 5.41 (d, ^3J = 7.9 Hz, 1H), 4.03 (t, ^3J = 5.5 Hz, 2H), 3.84 (s, 3H), 3.74−3.67 (m, 1H), 3.48−3.43 (m, 2H), 2.78−2.68 (m, 2H), 2.41−2.37 (m, 5H), 2.18−2.13 (m, 2H). ^{13}C NMR (125 MHz, $CDCl_3$): δ [ppm] = 171.2, 163.5, 163.2, 157.8, 156.3, 143.7, 138.0, 130.8, 130.0, 129.4, 127.3, 114.9, 103.5, 89.4, 64.8, 56.5, 51.9, 40.1, 39.7, 37.3, 28.4, 21.8. HPLC (10−90%): t_R = 15.95 min. MS (ESI): m/z (%) = 514.4 $[M + H]^+$. HR-MS (ESI) ($C_{26}H_{32}N_3O_6S^+$) calcd, 514.200 63; found, 514.199 02.

(*S*)-*N*-(4-(Hydroxyamino)-1-(4-(3-((4-methoxypyridin-2-yl)-amino)propoxy)phenyl)-4-oxobutan-2-yl)-4-isopropoxybenzamide (4). The Boc-deprotection and acylation of **8** (32.0 mg, 67.6 μmol) with 4-isopropoxybenzoic acid (14.6 mg, 81.1 μmol) followed GP1a. After formation of the hydroxamic acid according to GP2b, purification yielded compound **4** (2.35 mg, 4.72 μmol, 7%) as TFA salt. HPLC (10−90%): t_R = 17.93 min. MS (ESI): m/z (%) = 537.3 $[M + H]^+$. HR-MS (ESI) ($C_{29}H_{37}N_4O_6^+$) calcd, 537.270 76; found, 537.269 13.

(*S*)-*N*-Hydroxy-4-(4-(3-((4-methoxypyridin-2-yl)amino)-propoxy)phenyl)-3-((4-methylphenyl)sulfonamido)-butanamide (5). The Boc-deprotection and acylation of **8** (43.0 mg, 90.8 μmol) with 4-toluenesulfonyl chloride (20.8 mg, 0.11 mmol) followed GP1b. After formation of the hydroxamic acid according to GP2b, purification yielded compound **5** (4.36 mg, 8.25 μmol, 9%) as TFA salt. HPLC (10−90%, 30 min): t_R = 13.78 min. MS (ESI): m/z (%) = 529.3 $[M + H]^+$. HR-MS (ESI) ($C_{26}H_{33}N_4O_6S^+$) calcd, 529.211 53; found, 529.210 55.

(*S*)-3-(4-Fluorobenzamido)-4-(4-(3-((4-methoxypyridin-2-yl)-amino)propoxy)phenyl)butanoic Acid (6). The deprotection and acylation of the ligand precursor **8** (50 mg, 0.11 mmol) with 4-fluorobenzoic acid (18.2 mg, 0.13 mmol) followed GP1a. The crude product was deprotected according to GP2a. Purification yielded compound **6** (7.9.mg, 16.4 μmol, 15%) as TFA salt. ^{1}H NMR (500 MHz, DMSO): δ [ppm] = 12.77 (bs, 1H), 12.19 (bs, 1H), 8.34 (d, ^3J = 8.2 Hz, 1H), 8.18 (bs, 1H), 7.84 (d, ^3J = 8.4 Hz, 2H), 7.80 (d, ^3J = 7.1 Hz, 1H), 7.29 (d, ^3J = 8.8 Hz, 2H), 7.13 (d, ^3J = 8.5 Hz, 2H), 6.83 (d, ^3J = 8.8 Hz, 2H), 6.83 (d, ^3J = 8.8 Hz, 2H), 6.46 (d, ^3J = 6.3 Hz, 1H), 6.31 (s, 1H), 4.45−4.38 (m, 1H), 4.01 (t, ^3J = 5.9 Hz, 2H), 3.85 (s, 3H), 3.47−3.41 (m, 2H), 2.81−2.74 (m, 2H), 2.53−2.48 (m, 1H), 2.43 (dd, ^2J = 15.4 Hz, ^3J = 6.1 Hz, 1H), 2.03−1.96 (m, 2H). ^{13}C NMR (125 MHz, DMSO): δ [ppm] = 172.4, 169.0, 164.7, 162.8, 158.0, 157.1, 156.8, 131.1, 130.8, 130.1, 129.8, 115.2, 114.2, 103.9, 91.5, 64.6, 56.3, 48.5, 38.6, 27.9. HPLC (10−90%): t_R = 15.58 min. MS (ESI): m/z (%) = 482.4 $[M + H]^+$. HR-MS (ESI) ($C_{26}H_{29}FN_3O_5^+$) calcd, 482.208 58; found, 482.206 65.

3-((4-Methoxypyridin-2-yl)amino)propan-1-ol (7). 2-Amino-4-methoxypyridine (0.40 g, 3.22 mmol, 1 equiv) and 3-bromopropanol (1.34 g, 9.67 mmol, 3 equiv) were dissolved in DMF and heated up in a sealed glass tube to 80 °C for 48 h. The reaction mixture was purified by flash chromatography (DCM/MeOH 9:1 + 1% TEA) to give **7** as a pale yellow solid (0.54 g, 2.95 mmol, 92%). ^{1}H NMR (250 MHz, $CDCl_3$): δ [ppm] = 8.11 (s, 1H), 7.92 (d, ^3J = 7.5 Hz, 1H), 6.63−6.59 (dd, ^3J = 5.0, Hz, ^3J = 2.5 Hz, 1H), 6.40 (d, ^3J = 2.5 Hz, 1H), 4.76 (bs, 1H), 4.13 (t, ^3J = 7.5 Hz, 2H), 3.89 (s, 3H), 3.46−3.40 (m, 2H), 1.88−1.80 (m, 2H). HPLC (0−30%, 30 min): t_R = 15.05 min. MS (ESI): m/z = 183.1 $[M + H]^+$.

(*S*)-Methyl 3-(*tert*-Butoxycarbonyl)amino)-4-(4-(3-((4-methoxypyridin-2-yl)amino)propoxy)phenyl)butanoate (8). Compound **10** (550 mg of crude product) was dissolved in absolute DCM. Next, 2-amino-4-methoxypyridine (0.21 mg, 1.73 mmol) and magnesium sulfate monohydrate (0.87 mg, 6.27 mmol) were added. After the suspension was stirred for 1 h at room temperature, sodium triacetoxyborohydride (1.71 g, 8.07 mmol) was added, and stirring was continued overnight. After addition of 50 mL of a saturated $NaHCO_3$ solution and further 30 min of stirring, the organic layer was extracted twice with DCM (50 mL) and dried over Na_2SO_4. After filtration, the solution was concentrated to dryness and the crude product was purified by flash chromatography (DCM/EtOAc 1:1) to give **8** as a colorless oil (0.42 mg, 0.89 mmol, 62% over two steps). ^{1}H NMR (500 MHz, DMSO): δ [ppm] = 7.77 (d, ^3J = 5.8 Hz, 1H), 7.07 (d, ^3J = 8.5 Hz, 2H), 6.86−6.84 (m, 3H), 6.49 (t, ^3J = 5.5 Hz, 1H), 6.11 (dd, ^3J = 5.8 Hz, ^4J = 2.2 Hz, 1H), 5.94 (d, ^4J = 2.2 Hz, 1H), 3.99 (t, ^3J = 6.3 Hz, 2H), 3.92−3.85 (m, 1H), 3.69 (s, 3H), 3.54 (s, 3H), 3.36−3.32 (m, 2H), 2.65−2.56 (m, 2H), 2.37 (d, ^3J = 6.9 Hz, 2H), 1.96−1.90 (m, 2H), 1.32 (s, 9H). ^{13}C NMR (125 MHz, DMSO): δ [ppm] = 171.4, 166.0, 160.7, 157.1, 154.9, 148.7, 130.4, 130.2, 114.2, 100.9, 90.7, 77.7, 65.3, 54.6, 51.4, 49.5, 37.8, 28.9, 28.3. HPLC (10−90%): t_R = 19.15 min. MS (ESI): m/z (%) = 474.2 $[M + H]^+$, 418.3 $[M - {}^t\text{Bu} + H]^+$, 374.3 $[M - \text{Boc} + H]^+$.

(*S*)-Methyl 3-((*tert*-Butoxycarbonyl)amino)-4-(4-(3-hydroxypropoxy)phenyl)butanoate (9). A solution of *N*-Boc-β-tyrosine methyl ester[26] (0.52 mg, 1.68 mmol) and K_2CO_3 (0.58 mg, 4.20 mmol) in absolute DMF was stirred for 30 min at 0 °C. Next, 3-bromo-1-propanol (161 μL, 1.85 mmol) was added, and the mixture was stirred for 16 h while warming to room temperature. The solvent was evaporated in vacuo. The residue was taken up with 1 N HCl and extracted with EtOAc. The combined organic layers were treated with saturated NaCl, dried over Na_2SO_4, and concentrated to dryness. The crude product was purified by flash chromatography (DCM/EtOAc 3:1) to give **9** as a colorless oil (0.56 mg, 1.53 mmol, 91%). ^{1}H NMR (500 MHz, DMSO): δ [ppm] = 7.06 (d, ^3J = 8.5 Hz, 2H), 6.82 (d, ^3J = 8.3 Hz, 2H), 6.79 (d, ^3J = 8.6 Hz, 1H), 4.51 (bs, 1H), 3.98 (t, ^3J = 6.4 Hz, 2H), 3.93−3.85 (m, 1H), 3.54 (s, 3H), 3.33−3.29 (m, 2H), 2.63−2.59 (m, 2H), 2.38 (d, ^3J = 6.9 Hz, 2H), 1.86−1.80 (m, 2H), 1.32 (s, 9H). ^{13}C NMR (125 MHz, DMSO): δ [ppm] = 171.3, 157.1, 154.8, 130.2, 130.1, 114.1, 77.6, 64.4, 57.3, 51.3, 49.4, 38.8, 32.1, 28.2. HPLC (10−100%): t_R = 18.34 min. MS (ESI): m/z (%) = 757.1 $[2M + Na]^+$, 390.2 $[M + Na]^+$, 268.3 $[M - \text{Boc} + H]^+$.

(*S*)-Methyl 3-(*tert*-Butoxycarbonyl)amino)-4-(4-(3-oxopropoxy)phenyl)butanoate (10). Compound **9** (0.53 mg, 1.44 mmol) was dissolved in absolute DCM, and Dess−Martin periodinane (1.83 g 4.32 mmol) was added in three portions within 1.5 h. The suspension was stirred for an additional 2 h at room temperature and extracted twice with a mixture of 10% sodium thiosulfate solution and saturated $NaHCO_3$ solution (1:1). The organic layers were combined, washed with H_2O and saturated NaCl, and dried over Na_2SO_4. The solvent was evaporated in vacuo, and compound **10** was obtained as a yellow oil (550 mg). The compound was used directly in the next step without further purification. ^{1}H NMR (360 MHz, DMSO): δ [ppm] = 9.72 (t, ^3J = 1.7 Hz, 1H), 7.08 (d, ^3J = 8.6 Hz, 2H), 6.84 (d, ^3J = 8.5 Hz, 2H), 6.80 (d, ^3J = 8.9 Hz, 1H), 4.24 (t, ^3J = 5.9 Hz, 2H), 3.94−3.82 (m, 1H), 3.54 (s, 3H), 2.87−2.83 (m, 2H), 2.64−2.35 (m, 2H), 2.44−2.33 (m, 2H), 1.32 (s, 9H). ^{13}C NMR (90 MHz, DMSO): δ [ppm] = 201.8, 171.3, 156.7, 154.8, 130.7, 130.1, 114.2, 77.6, 61.5, 51.3, 49.3, 42.7, 28.2. HPLC (10−90%): t_R = 21.91 min. MS (ESI): m/z (%) = 388.1 $[M + Na]^+$, 332.3 $[M - {}^t\text{Bu} + Na]^+$, 266.1 $[M - \text{Boc} + H]^+$.

■ ASSOCIATED CONTENT

Ⓢ Supporting Information

Competitive solid-phase integrin binding assay, activity profile of compound **2**, and docking methods. This material is available free of charge via the Internet at http://pubs.acs.org.

AUTHOR INFORMATION

Corresponding Author

*Phone: +49 (0)89 289 13300. Fax: +49 (0)89 289 13210. E-mail: kessler@tum.de.

Present Addresses

[#]S.N.: Department of New Materials and Biosystems, Max Planck Institute for Intelligent Systems, Heisenbergstrasse 3, 70569 Stuttgart, Germany.

[∞]C.M.-M.: Biomaterials, Biomechanics and Tissue Engineering Group, Department of Materials Science and Metallurgical Engineering, Technical University of Catalonia (UPC), Av. Diagonal 647, E08028 Barcelona, Spain.

Author Contributions

[×]S.N. and F.R. contributed equally.

The manuscript was written through contributions of all authors. All authors have given approval to the final version of the manuscript.

Notes

The authors declare no competing financial interest.

ACKNOWLEDGMENTS

We thank CompInt (Materials Science of Complex Interfaces) of the Elite Network of Bavaria, IGSSE (International Graduate School of Science and Engineering) and Bund der Freunde der TU München e.V. for funding, IAS (Institute for Advanced Study) of Technische Universität München, CIPSM (Center for Integrated Protein Science Munich), and Max Planck Society for financial support. We gratefully thank King Abdulaziz University (KAU) for technical and financial support (Grant HiCi/25-3-1432).

ABBREVIATIONS USED

ECM, extracellular matrix; ELISA, enzyme-linked immunosorbent assay; MIDAS, metal-ion-dependent adhesion site; HATU, *O*-(7-azabenzotriazol-1-yl)-*N*,*N*,*N*′,*N*′-tetramethyluronium hexafluorophosphate

REFERENCES

(1) Goodman, S. L.; Picard, M. Integrins as therapeutic targets. *Trends Pharmacol. Sci.* **2012**, *33*, 405−412.

(2) Kapp, T. G.; Rechenmacher, F.; Sobahi, T. R.; Kessler, H. Integrin modulators: a patent review. *Expert Opin. Ther. Pat.* **2013**, *23*, 1273−1295.

(3) Desgrosellier, J. S.; Cheresh, D. A. Integrins in cancer: biological implications and therapeutic opportunities. *Nat. Rev. Cancer* **2010**, *10*, 9−22.

(4) Shattil, S. J.; Kim, C.; Ginsberg, M. H. The final steps of integrin activation: the end game. *Nat. Rev. Mol. Cell Biol.* **2010**, *11*, 288−300.

(5) Pierschbacher, M. D.; Ruoslahti, E. Cell attachment activity of fibronectin can be duplicated by small synthetic fragments of the molecule. *Nature* **1984**, *309*, 30−33.

(6) Hynes, R. O. A reevaluation of integrins as regulators of angiogenesis. *Nat. Med.* **2002**, *8*, 918−921.

(7) Marelli, U. K.; Rechenmacher, F.; Sobahi, T. R.; Mas-Moruno, C.; Kessler, H. Tumor targeting via integrin ligands. *Front. Oncol.* **2013**, *3*, 222.

(8) Aumailley, M.; Gurrath, M.; Müller, G.; Calvete, J.; Timpl, R.; Kessler, H. Arg-Gly-Asp constrained within cyclic pentapeptides. Strong and selective inhibitors of cell adhesion to vitronectin and laminin fragment P1. *FEBS Lett.* **1991**, *291*, 50−54.

(9) Haubner, R.; Finsinger, D.; Kessler, H. Stereoisomeric peptide libraries and peptidomimetics for designing selective inhibitors of the $\alpha_v\beta_3$ integrin for a new cancer therapy. *Angew. Chem., Int. Ed.* **1997**, *36*, 1374−1389.

(10) Dechantsreiter, M. A.; Planker, E.; Mathä, B.; Lohof, E.; Hölzemann, G.; Jonczyk, A.; Goodman, S. L.; Kessler, H. N-Methylated cyclic RGD peptides as highly active and selective $\alpha_v\beta_3$ integrin antagonists. *J. Med. Chem.* **1999**, *42*, 3033−3040.

(11) Dayam, R.; Aiello, F.; Deng, J.; Wu, Y.; Garofalo, A.; Chen, X.; Neamati, N. Discovery of small molecule integrin $\alpha_v\beta_3$ antagonists as novel anticancer agents. *J. Med. Chem.* **2006**, *49*, 4526−4534.

(12) Heckmann, D.; Meyer, A.; Marinelli, L.; Zahn, G.; Stragies, R.; Kessler, H. Probing integrin selectivity: rational design of highly active and selective ligands for the $\alpha5\beta1$ and $\alpha v\beta3$ integrin receptor. *Angew. Chem., Int. Ed.* **2007**, *46*, 3571−3574.

(13) Zanardi, F.; Burreddu, P.; Rassu, G.; Auzzas, L.; Battistini, L.; Curti, C.; Sartori, A.; Nicastro, G.; Menchi, G.; Cini, N.; Bottonocetti, A.; Raspanti, S.; Casiraghi, G. Discovery of subnanomolar arginine-glycine-aspartate-based $\alpha_V\beta_3/\alpha_V\beta_5$ integrin binders embedding 4-aminoproline residues. *J. Med. Chem.* **2008**, *51*, 1771−1782.

(14) Gentilucci, L.; Cardillo, G.; Spampinato, S.; Tolomelli, A.; Squassabia, F.; De Marco, R.; Bedini, A.; Baiula, M.; Belvisi, L.; Civera, M. Antiangiogenic effect of dual/selective $\alpha_5\beta_1/\alpha_v\beta_3$ integrin antagonists designed on partially modified retro-inverso cyclotetrapeptide mimetics. *J. Med. Chem.* **2010**, *53*, 106−118.

(15) Corti, A.; Curnis, F. Tumor vasculature targeting through NGR peptide-based drug delivery systems. *Curr. Pharm. Biotechnol.* **2011**, *12*, 1128−1134.

(16) Bianchini, F.; Cini, N.; Trabocchi, A.; Bottoncetti, A.; Raspanti, S.; Vanzi, E.; Menchi, G.; Guarna, A.; Pupi, A.; Calorini, L. ^{125}I-Radiolabeled morpholine-containing arginine-glycine-aspartate (RGD) ligand of $\alpha_v\beta_3$ integrin as a molecular imaging probe for angiogenesis. *J. Med. Chem.* **2012**, *55*, 5024−5033.

(17) Colombo, R.; Mingozzi, M.; Belvisi, L.; Arosio, D.; Piarulli, U.; Carenini, N.; Perego, P.; Zaffaroni, N.; De Cesare, M.; Castiglioni, V.; Scanziani, E.; Gennari, C. Synthesis and biological evaluation (in vitro and in vivo) of cyclic arginine-glycine-aspartate (RGD) peptidomimetic-paclitaxel conjugates targeting integrin $\alpha_V\beta_3$. *J. Med. Chem.* **2012**, *55*, 10460−10474.

(18) Mas-Moruno, C.; Rechenmacher, F.; Kessler, H. Cilengitide: the first anti-angiogenic small molecule drug candidate. Design, synthesis and clinical evaluation. *Anti-Cancer Agents Med. Chem.* **2010**, *10*, 753−768.

(19) Reardon, D. A.; Cheresh, D. Cilengitide: a prototypic integrin inhibitor for the treatment of glioblastoma and other malignancies. *Genes Cancer* **2011**, *2*, 1159−1165.

(20) Merck KGaA press release, February 25, 2013: http://www.merckgroup.com/en/media/extNewsDetail.html?newsId=BE2FE07AD630830EC1257B1D001F007B&newsType=1.

(21) Bochen, A.; Marelli, U. K.; Otto, E.; Pallarola, D.; Mas-Moruno, C.; Di Leva, F. S.; Boehm, H.; Spatz, J. P.; Novellino, E.; Kessler, H.; Marinelli, L. Biselectivity of isoDGR peptides for fibronectin binding integrin subtypes $\alpha5\beta1$ and $\alpha v\beta6$: conformational control through flanking amino acids. *J. Med. Chem.* **2013**, *56*, 1509−1519.

(22) Mondal, G.; Barui, S.; Chaudhuri, A. The relationship between the cyclic-RGDfK ligand and $\alpha v\beta3$ integrin receptor. *Biomaterials* **2013**, *34*, 6249−6260.

(23) Pfaff, M.; Tangemann, K.; Müller, B.; Gurrath, M.; Müller, G.; Kessler, H.; Timpl, R.; Engel, J. Selective recognition of cyclic RGD peptides of NMR defined conformation by αIIbβ3, αVβ3, and $\alpha5\beta1$ integrins. *J. Biol. Chem.* **1994**, *269*, 20233−20238.

(24) Marinelli, L.; Meyer, A.; Heckmann, D.; Lavecchia, A.; Novellino, E.; Kessler, H. Ligand binding analysis for human $\alpha5\beta1$ integrin: strategies for designing new $\alpha5\beta1$ integrin antagonists. *J. Med. Chem.* **2005**, *48*, 4204−4207.

(25) Smallheer, J. M.; Weigelt, C. A.; Woerner, F. J.; Wells, J. S.; Daneker, W. F.; Mousa, S. A.; Wexler, R. R.; Jadhav, P. K. Synthesis and biological evaluation of nonpeptide integrin antagonists containing spirocyclic scaffolds. *Bioorg. Med. Chem. Lett.* **2004**, *14*, 383−387.

(26) Heckmann, D.; Meyer, A.; Laufer, B.; Zahn, G.; Stragies, R.; Kessler, H. Rational design of highly active and selective ligands for the $\alpha5\beta1$ integrin receptor. *ChemBioChem* **2008**, *9*, 1397−1407.

(27) Marinelli, L.; Lavecchia, A.; Gottschalk, K.-E.; Novellino, E.; Kessler, H. Docking studies on αvβ3 integrin ligands: pharmacophore refinement and implications for drug design. *J. Med. Chem.* **2003**, *46*, 4393−4404.
(28) Rechenmacher, F.; Neubauer, S.; Polleux, J.; Mas-Moruno, C.; De Simone, M.; Cavalcanti-Adam, E. A.; Spatz, J. P.; Fässler, R.; Kessler, H. Functionalizing αvβ3- or α5β1-selective integrin antagonists for surface coating: a method to discriminate integrin subtypes in vitro. *Angew. Chem., Int. Ed.* **2013**, *52*, 1572−1575.
(29) Rahmouni, S.; Lindner, A.; Rechenmacher, F.; Neubauer, S.; Sobahi, T. R.; Kessler, H.; Cavalcanti-Adam, E. A.; Spatz, J. P. Hydrogel micropillars with integrin selective peptidomimetic functionalized nanopatterned tops: a new tool for the measurement of cell traction forces transmitted through $\alpha_v\beta_3$- or $\alpha_5\beta_1$-integrins. *Adv. Mater.* **2013**, *25*, 5869−5874.
(30) Neubauer, S.; Rechenmacher, F.; Beer, A. J.; Curnis, F.; Pohle, K.; D'Alessandria, C.; Wester, H.-J.; Reuning, U.; Corti, A.; Schwaiger, M.; Kessler, H. Selective imaging of the angiogenic relevant integrins α5β1 and αvβ3. *Angew. Chem., Int. Ed.* **2013**, *52*, 11656−11659.
(31) Wang, J.; Breslin, M. J.; Coleman, P. J.; Duggan, M. E.; Hunt, C. A.; Hutchinson, J. H.; Leu, C.-T.; Rodan, S. B.; Rodan, G. A.; Duong, L. T.; Hartman, G. D. Non-peptide $\alpha_v\beta_3$ antagonists. Part 7: 3-Substituted tetrahydro-[1,8]naphthyridine derivatives. *Bioorg. Med. Chem. Lett.* **2004**, *14*, 1049−1052.
(32) Stragies, R.; Osterkamp, F.; Zischinsky, G.; Vossmeyer, D.; Kalkhof, H.; Reimer, U.; Zahn, G. Design and synthesis of a new class of selective integrin α5β1 antagonists. *J. Med. Chem.* **2007**, *50*, 3786−3794.
(33) Knör, S.; Khrenov, A. V.; Laufer, B.; Saenko, E. L.; Hauser, C. A. E.; Kessler, H. Development of a peptidomimetic ligand for efficient isolation and purification of factor VIII via affinity chromatography. *J. Med. Chem.* **2007**, *50*, 4329−4339.
(34) Frank, A. O.; Otto, E.; Mas-Moruno, C.; Schiller, H. B.; Marinelli, L.; Cosconati, S.; Bochen, A.; Vossmeyer, D.; Zahn, G.; Stragies, R.; Novellino, E.; Kessler, H. Conformational control of integrin-subtype selectivity in isoDGR peptide motifs: a biological switch. *Angew. Chem., Int. Ed.* **2010**, *49*, 9278−9281.
(35) Rechenmacher, F.; Neubauer, S.; Mas-Moruno, C.; Dorfner, P. M.; Polleux, J.; Guasch, J.; Conings, B.; Boyen, H.-G.; Bochen, A.; Sobahi, T. R.; Burgkart, R.; Spatz, J. P.; Fässler, R.; Kessler, H. A molecular toolkit for the functionalization of titanium-based biomaterials that selectively control integrin-mediated cell adhesion. *Chem.—Eur. J.* **2013**, *19*, 9218−9223.
(36) Humphries, M. Integrin structure. *J. Biochem. Soc. Trans.* **2000**, *28*, 311−339.
(37) Heckmann, D.; Laufer, B.; Marinelli, L.; Limongelli, V.; Novellino, E.; Zahn, G.; Stragies, R.; Kessler, H. Breaking the dogma of the metal-coordinating carboxylate group in integrin ligands: introducing hydroxamic acids to the MIDAS to tune potency and selectivity. *Angew. Chem., Int. Ed.* **2009**, *48*, 4436−4440.
(38) Ho, C. Y.; Strobel, E.; Ralbovsky, J.; Galemmo, R. A. Improved solution- and solid-phase preparation of hydroxamic acids from esters. *J. Org. Chem.* **2005**, *70*, 4873−4875.
(39) Hackel, B. J.; Kimura, R. H.; Miao, Z.; Liu, H.; Sathirachinda, A.; Cheng, Z.; Chin, F. T.; Gambhir, S. S. ^{18}F-Fluorobenzoate-labeled cystine knot peptides for PET imaging of integrin $\alpha_v\beta_6$. *J. Nucl. Med.* **2013**, *54*, 1101−1105.
(40) Schottelius, M.; Laufer, B.; Kessler, H.; Wester, H.-J. Ligands for mapping $\alpha_v\beta_3$-integrin expression in vivo. *Acc. Chem. Res.* **2009**, *42*, 969−980.
(41) Xiong, J.-P.; Stehle, T.; Zhang, R.; Joachimiak, A.; Frech, M.; Goodman, S. L.; Arnaout, M. A. Crystal structure of the extracellular segment of integrin αvβ3 in complex with an Arg-Gly-Asp ligand. *Science* **2002**, *296*, 151−155.
(42) Gottlieb, H. E.; Kotlyar, V.; Nudelman, A. NMR chemical shifts of common laboratory solvents as trace impurities. *J. Org. Chem.* **1997**, *62*, 7512−7515.